Determination of phase transition points of ionic liquids by combination of thermal analysis and conductivity measurements at very low heating and cooling rates

Philipp Wachter, Christian Schreiner, Hans-Georg Schweiger, Heiner Jakob Gores *

Workgroup Electrochemistry and Electrolytes, Institute of Physical and Theoretical Chemistry, University of Regensburg, Universitaetsstr. 31, D-93040 Regensburg, Germany

ABSTRACT

The determination of phase transition points of nine different ionic liquids (ILs) was performed by thermal analysis with simultaneous recording of conductivity. Conductivity of electrolyte solutions and ILs drastically changes during phase transitions and thus is an additional and very sensitive indicator for measuring phase transition points. Evaluation of temperature–time functions and conductivity–time functions with our computer-coupled automated equipment enabled the determination of melting temperatures with high accuracy and reliability. This claim is based on large samples, low temperature change rates and by regularly repeated measurements, *i.e.* at least seven measurements per IL. The melting temperatures of 1-butyl-1-methylpyrrolidinium trifluoromethanesulfonate, 1-butyl-1-methylpyrrolidinium tris(penta-fluoroethyl)trifluorophosphate, and 1-methyl-3-propylimidazolium iodide were, to our knowledge, determined for the first time. The melting temperatures of the other 1-butyl-1-methylpyrrolidinium-, 1-ethyl-3-methylimidazolium-, 1-hexyl-3-methylimidazolium-, and trimethylsulfonium-based ILs showed either a very good accordance with values published in literature or were distinctly higher.

© 2010 Elsevier Ltd. All rights reserved.

1. Introduction

In recent years, ionic liquids (ILs) were often considered and studied as substitutes for common organic solvents in electrolyte solutions for various technical applications. For the majority of those applications, phase transition temperatures play an important role. For example, the operating range of several electrochemical devices for energy storage and transformation, such as lithium-ion batteries, double layer capacitors, and photo-electrochemical or dye-sensitized solar cells is limited by the crystallization temperature of the applied electrolyte. Therefore, the knowledge of precise liquid to solid phase transition temperatures plays an essential role in the formulation of those electrolytes.

The favourable properties of ILs include high conductivity and ionic strength, negligible vapour pressure, and high thermal, chemical, and electrochemical stability. On the other hand, ILs generally tend to strong supercooling rendering the determination of liquid to solid phase transition temperatures much more difficult than for organic solvents.

Phase transition points of common imidazolium based ILs measured by differential scanning calorimetry (DSC) are frequently reported [1–7]. Only few or no data have been published for ILs with tendency to strong supercooling, since in combination with the generally applied high cooling and heating rates and resulting short time scales, no crystallization of those ILs occurs within the working range of common DSC devices. Therefore, often only glass-transition points are determined. These transitions at comparatively low temperatures often lead to the wrong assumption of extremely broad liquid ranges for specific ILs, as later shown for 1-methyl-3-propylimidazolium iodide (MPII), a frequently applied IL for the formulation of electrolytes for dye-sensitized solar cells (DSSCs).

2. Experimental

2.1. Materials

The ILs examined during this study were either synthesized according to reference [8] or obtained from Merck. The NMR data (^{1}H, ^{13}C, ^{11}B, ^{19}F) of all examined ILs did not show any impurities. Water contents of the ILs were determined via Karl-Fischer titration using a DL 18 titrator from Mettler (Giessen, Germany). Prior to the measurements, all ILs were dried under high vacuum (10^{-3} Pa) and if necessary at elevated temperatures (up to 333 K) to get a mass fraction of water below 10^{-4}. Water contents, sources and purity grades of the ILs are summarized in table 1.

---

* Corresponding author. Tel.: +49 941 943 4746/+49 9402 8040; fax: +49 9402 8035.

E-mail address: Heiner.Gores@Chemie.Uni-Regensburg.de (H.J. Gores).

TABLE 1
Investigated materials with corresponding acronyms, water contents, and source with given purity grade.

Acronym	Material	$10^6\,w$	Source/ purity grade
BMPINTf$_2$	1-Butyl-1-methylpyrrolidinium bis(trifluoromethylsulfonyl)imide	18	Merck *ultra pure*
BMPIOTf	1-Butyl-1-methylpyrrolidinium trifluoromethanesulfonate		Merck *high purity*
BMPIFAP	1-Butyl-1-methylpyrrolidinium tris(penta-fluoroethyl)trifluorophosphate	41	Merck *high purity*
EMIDCA	1-Ethyl-3-methylimidazolium dicyanamide	20	[a]
EMIBF$_4$	1-Ethyl-3-methylimidazolium tetrafluoroborate	23	[a]
EMINTf$_2$	1-Ethyl-3-methylimidazolium bis(trifluoromethylsulfonyl)imide	21	[a]
HMINTf$_2$	1-Hexyl-3-methylimidazolium bis(trifluoromethylsulfonyl)imide	52	Merck *ultra pure*
MPII	1-Methyl-3-propylimidazolium iodide	75	[a]
Me$_3$SDCA	Trimethylsulfonium dicyanamide		[b]

w = mass fraction of water as determined by Karl-Fischer titration.
[a] Synthesized according to reference [8].
[b] Provided by Dirk Gerhard, Friedrich-Alexander-Universität Erlangen-Nürnberg (Germany).

2.2. Apparatus and measurements

The temperature of the ILs was measured with a home-built fast multi-channel precision thermometer [9,10] with simultaneous recording of conductivity by a thereto coupled home-built multi-channel precision conductometer [11]. The applied thermostat-cryostat assembly and $G(t)$–$T(t)$-measuring cells with appropriate stirring devices are described in detail in references [9–11]. With this measurement setup, accurate temperature and conductivity measurements were feasible over the temperature range from (193 to 338) K at precisely adjustable cooling and heating rates ranging from (±2.5 to ±30) K · h^{-1}. The $G(t)$–$T(t)$-measuring cells were filled and sealed gastight in a glove box under an argon atmosphere and then transferred to the stirring device already placed in the thermostat bath. In order to reduce the impact of statistical outliers and due to often inhibited crystallization by strongly pronounced supercooling, every sample was cooled down and heated up for at least seven to 20 times. Thus, crystallization and melting temperatures and their errors could be determined with satisfying accuracy and known statistical error. The accuracy and reliability of the measuring method and equipment have been shown in reference [10] by determination of phase transition points of frequently examined organic solvents and their comparison with literature values.

As mentioned above, for this work the conductivity was exclusively determined to obtain an additional indicator for phase transition points. For further evaluation of the conductivity data, *e.g.* with respect to temperature dependence, a time consuming calibration of the measurement cells would have been necessary.

Generally, the crystallization point is defined as the temperature of the halt obtained during crystallization of the sample [10] upon cooling. For ILs, this halt is often very short due to strong supercooling. Therefore, instead of determination by extrapolation of the almost horizontal halt and the cooling branch with subsequent calculation of the intersection point, the crystallization point is defined as highest temperature reached during crystallization [12]. The actual supercooling that occurred was defined as the temperature difference between the melting temperature and the temperature where the sample starts to crystallize. Upon cooling, the conductivity of the samples often inclined to zero prior to crystal-
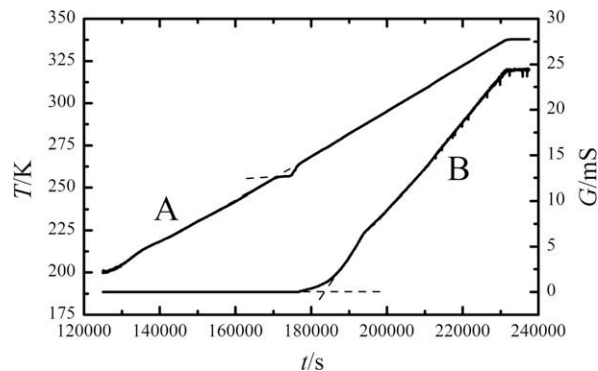

FIGURE 1. Determination of the melting temperature of EMINTf$_2$ by evaluation of temperature and conductivity recorded at a heating rate of 5 K · h^{-1}. Plot of temperature T (A) and conductivity G (B) *versus* time and extrapolation of the linear parts (- - -) for determination of the melting temperature.

lization due to supercooling and insufficient sensitivity of the measuring equipment. Therefore, evaluation of $G(t)$-curves and ln G-plots was performed exclusively with respect to the determination of melting temperatures. The determination of the melting temperature of EMINTf$_2$ by evaluation of the heating branches of the $T(t)$- and $G(t)$-curves is illustrated in figure 1. In both cases, the melting temperature is defined as the intersection point of the extrapolated linear parts of the curve before and after melting. Evaluation of ln G-plots with respect to melting temperatures was performed in an identical manner.

3. Results and discussion

The influence of cooling and heating rates on the measurement of crystallization and melting temperatures of organic solvents has been discussed in reference [10]. Generally no valid conclusion of the effect of varying cooling and heating rates can be given for ILs. The most uniform behaviour was found for the melting temperatures T_m that generally decrease slightly with increasing heating rate, as shown in figure 2 for Me$_3$SDCA and EMIDCA. The determined crystallization points T_c generally decreased slightly with increasing cooling rate, as shown in figure 3 for EMINTf$_2$.

In contrast to the melting temperatures obtained from $T(t)$-curves, no distinct tendency with increasing heating rate could be observed for melting temperatures obtained by evaluation of conductivity data, as shown in figure 4 for EMIDCA. Generally, phase transition points obtained from $T(t)$-curves and from conductivity data showed the best accordance at comparatively low cooling and heating rates. Due to that and due to a lower percentage of ILs crystallizing at high rather than at low cooling rates, the majority of measurements was finally conducted at a fixed low cooling and heating rate v of ±5 K · h^{-1}.

The mean values of the melting temperatures determined by evaluation of $T(t)$- and $G(t)$-curves and ln G-plots are listed in table 3 along with the corresponding standard deviations. Additionally, the mean values of the differences between the
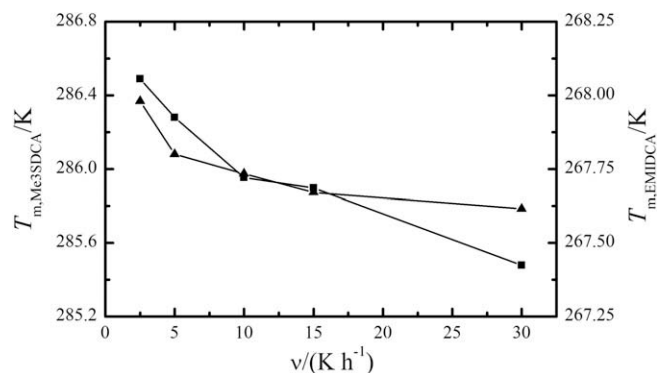

FIGURE 2. Melting temperatures T_m of Me$_3$SDCA (■) and EMIDCA (▲) as function of the applied heating rate v. Continuous lines are guides to the eye.